Eur. Phys. J. B **19**, 589–597 (2001)

THE EUROPEAN PHYSICAL JOURNAL B

EDP Sciences

Low frequency and weakly nonlinear spin transport in ferromagnet/insulator single and double junctions

Zheng-Chuan Wang, Qing-Rong Zheng, Gang Su[a], and Bao-Heng Zhao

Department of Physics, Graduate School at Beijing, University of Science and Technology of China, Chinese Academy of Sciences, PO Box 3908, Beijing 100039, PR China

Received 1st September 2000 and Received in final form 5 December 2000

Abstract. In this paper, we apply Büttiker's gauge invariant, charge conservation, nonlinear transport theory to explore the spin-polarized tunneling of ferromagnet/insulator (semiconductor) single and double junctions. The Green function of spin-polarized tunneling is calculated by the tight-binding approximation method. The energy and the angle (between the molecular field and the vertical axis) dependences of the weakly nonlinear dc transport coefficient and the linear low frequency ac transport coefficient are investigated. The ac tunneling magnetoresistance is also discussed.

PACS. 75.70.Cn Interfacial magnetic properties (multilayers, magnetic quantum wells, superlattices, magnetic heterostructures) – 73.40.Rw Metal-insulator-metal structures – 73.23.Hk Coulomb blockade; single-electron tunneling

1 Introduction

Recently, the spin-polarized tunneling through ferromagnet/insulator (semiconductor)/ferromagnet (FM/I(S)/FM) junction has attracted much more attention [1–4]. Several experiments have been done to measure the tunneling conductance and magnetoresistance of the FM/I(S)/FM junctions. Not only the spin-polarized tunneling has prospective use as high-density, nonvolatile storage media or as a field sensor, but also it play an important role in the study of giant magnetoresistance (GMR) effect of multilayers. In 1989, Slonczewski [5] proposed a free electron model to analyze the transmission of charge and spin currents flowing through a nonmagnetic electron tunneling barrier separating two ferromagnetic conductors. Following this model, Zhang *et al.* [6,7] further studied the tunneling through ferromagnet/insulator (semiconductor) single and double junctions subject to a dc bias. Based on Landauer-Büttiker formalism, Bauer [8] presented a perpendicular transport theory for the metallic multilayers. In the absence of spin-flip relaxation process, it unities the different results of previous approaches. They also applied it to discuss the magnetoresistance of antiferromagnetically coupled magnetic multilayers. Besides the ferromagnet/insulator/ferromagnet junction, the ferromagnet/normal metal/ferromagnet junction is also explored. Inspired by the circuit theory of Andreev reflection, Brataas *et al.* [9] formulate a finite-element transport theory for spin transport in a ferromagnet-normal metal system. In the presence of ferromagnetic order, a contact can be described by four conductance parameters. This theory considerably simplifies the calculation of transport properties of complicated ferromagnet-normal metal system.

However, the known spin tunneling models [5–7] are based on the free electron approximation, in which electron-electron correlations due to long ranged Coulombic interaction are not taken into account. When the external bias is varied, the time dependence of internal electric potential which originates from electron-electron interactions will induce a displacement current. Therefore, the total current in time dependent transport should be composed of two parts, namely, the displacement current and the particle current. It is this total current to count experiments, not just the particle current. Since electron-electron correlations in the free electron approximation are neglected, the displacement current is omitted and only is the particle current calculated in these theories such that the gauge invariance and current conservation, which are fundamental requirements of the physical principles, may not be kept. The nonlinear effect on spin-polarized tunneling problems considered in previous models is clearly incorrect because those theories do not obey the gauge invariance. On the other hand, the theories proposed to explain the experimental results only deal with the dc transport of spin-dependent transmission. It is clear that the research on ac properties of spin-dependent transport is very important both in application and in fundamental sense, while there are few researchers to pay attention to the problem of the spin-polarized tunneling with ac bias.

Büttiker and coworkers [10–12] proposed a transport theory in the frame of the scattering matrix approach to explain both the dc and ac electrical conductance in mesoscopic systems. In their formalism, the conservation of the overall charge and current as well

[a] e-mail: gs1966@sina.com

as the invariance under a global voltage shift (gauge invariance) are emphasized. In this paper, we shall extend Büttiker′s formalism to the case in which the spin degree of freedom is stressed, and apply the theory to spin polarized tunneling of ferromagnet/insulator (semiconductor) single and double junctions. Because a general time dependent nonlinear transport problem is very difficult to handle, we only consider the weakly nonlinear dc-transport and linear low frequency spin-polarized tunneling transport. The Green function needed in the spin-polarized tunneling transport theory is calculated by use of the tight-binding approximation method (or the method of finite difference) [13]. The basic formalism concerning the weakly nonlinear dc and linear low frequency conductance of tunneling junctions are described in Section 2. In Section 3, we shall present our numerical analyses on the tunneling of FM/I(S) single and double junctions. Finally, a brief summary is given in Section 4.

2 Formalism

Consider FM/I(S)/.../FM/.../I(S)/FM multilayers which are connected by two electron reservoirs at contacts $\alpha = 1, 2$ with voltage V_α. We will use Büttiker's scattering approach to investigate this system. Büttiker's scattering approach has been successfully applied to many interesting mesoscopic systems [14–19]. The salient point of this theory is the conservation of the overall charge and current as well as the invariance under a global voltage shift (gauge invariance). The transport properties of the system are described by the scattering matrix $S_{\alpha s\beta s'}$ which relates the outgoing current amplitude at contact α with spin s to the incident current amplitude at contact β with spin s'. According to Büttiker's approach [10–12], the electric current through contact α is given by

$$I_\alpha = \frac{2e}{h}\sum_{\beta=1}^{N}\int \mathrm{d}E f(E - E_\mathrm{F} - eV_\beta)\sum_{s,s'} A_{\alpha s,\beta s'}(E), \quad (1)$$

where $f(z) = [1 + \exp(z/k_\mathrm{B}T)]^{-1}$ is the Fermi function, and $A_{\alpha s,\beta s'}(E) = \delta_{\alpha\beta}\delta_{ss'} - S^{+}_{\alpha s,\beta s'}(E)S_{\alpha s,\beta s'}(E)$. To obtain weakly nonlinear transport, equation (1) is expanded with respect to the voltage V_α as

$$I_\alpha = \sum_\beta G_{\alpha\beta}(0)V_\beta + \sum_{\beta\gamma} G_{\alpha\beta\gamma}(0)V_\beta V_\gamma + \cdots, \quad (2)$$

where the linear coefficient is defined as

$$G_{\alpha\beta}(0) = \frac{e^2}{h}\int \mathrm{d}E(-\partial_E f)\sum_{s,s'} A_{\alpha s,\beta s'}(E), \quad (3)$$

and the weakly nonlinear coefficient is

$$G_{\alpha\beta\gamma}(0) = \frac{e^3}{h}\int \mathrm{d}E(-\partial_E f) \times \sum_{s,s'}\int \mathrm{d}x \frac{\delta A_{\alpha s,\beta s'}(E)}{\delta eU(x)}(2u_\gamma(x) - \delta_{\beta\gamma}), \quad (4)$$

with

$$\frac{\delta A_{\alpha s\beta t}}{\delta eU(x)} = -\left(S^{\dagger}_{\alpha s\beta t}\frac{\delta S_{\alpha s\beta t}}{\delta eU(x)} + \frac{\delta S^{\dagger}_{\alpha s\beta t}}{\delta eU(x)}S_{\alpha s\beta t}\right), \quad (5)$$

$U(x)$ is the internal electric potential, and $u_\gamma(x)$ is the characteristic potential determined by the following Poisson equation

$$-\partial_{xx}u_\alpha(x) + 4\pi e^2\int \mathrm{d}x' \Pi(x, x')u_\alpha(x') = 4\pi e^2\frac{\mathrm{d}n_\alpha(x)}{\mathrm{d}E}. \quad (6)$$

Here, we note that the spin degree of freedom does not explicitly appear in equation (6), so the formalism for the weakly nonlinear transport and the low frequency ac transport with spin will be formally the same as that without spin, although Green′s function and the scattering matrix are spin dependent. In equation (6), $\frac{\mathrm{d}n_\alpha(x)}{\mathrm{d}E} = \sum_\beta \frac{\mathrm{d}n_{\alpha\beta}(x)}{\mathrm{d}E}$ and

$$\frac{\mathrm{d}n_{\alpha\beta}(x)}{\mathrm{d}E} = -\frac{1}{4\pi\mathrm{i}}\sum_{st}\left(S^{\dagger}_{\alpha s,\beta t}\frac{\delta S_{\alpha s,\beta t}}{\delta U(x)} - \frac{\delta S^{\dagger}_{\alpha s,\beta t}}{\delta U(x)}S_{\alpha s,\beta t}\right) \quad (7)$$

is the partial local density of states. The sum over all contacts α, β gives the local density of states $\mathrm{d}n(x)/\mathrm{d}E$. $\Pi(x, x')$ is the Lindhard polarization function which can be simplified in the Thomas-Fermi approximation as

$$\Pi(x, x') = \frac{\mathrm{d}n(x)}{\mathrm{d}E}\delta(x - x'). \quad (8)$$

If the quasi-neutrality condition is used, the characteristic equation becomes an algebra equation

$$u_\alpha(x) = \frac{\mathrm{d}n_\alpha(x)}{\mathrm{d}E}\Big/\frac{\mathrm{d}n(x)}{\mathrm{d}E}, \quad (9)$$

which is reasonable if the characteristic potential is a slowly varying function of coordinates. We shall assume it for convenience in our subsequent calculation.

According to the Fisher-Lee relation, the scattering matrix with spin polarization can be expressed by Green's function $G_{\sigma\sigma'}(x, x')$ as

$$S_{\alpha\sigma,\beta\sigma'} = -\delta_{\alpha\beta}\delta_{\sigma\sigma'} + \mathrm{i}\sqrt{v_\alpha v_\beta}G_{\sigma\sigma'}(x_\alpha, x_\beta), \quad (10)$$

where $v = \frac{1}{\hbar}\frac{\partial E}{\partial k}$, k is the wave vector. Substituting the above equation into the partial local density of states, we can express it as

$$\frac{\mathrm{d}n_{\alpha\beta}(x)}{\mathrm{d}E} = -\frac{\sqrt{v_\alpha v_\beta}}{4\pi} \times \sum_{st}\left(S^{\dagger}_{\alpha s,\beta t}\frac{\delta G_{st}(x_\alpha, x_\beta)}{\delta U(x)} + \frac{\delta G^{\dagger}_{st}(x_\alpha, x_\beta)}{\delta U(x)}S_{\alpha s,\beta t}\right). \quad (11)$$

$$E - H_{\rm c} - \Sigma = \begin{pmatrix} E-\alpha_1-\Sigma_1 & -\beta_1 & 0 & 0 & 0 & 0 \\ -\beta_1 & E-\alpha_2 & -\beta_2 & 0 & 0 & 0 \\ 0 & -\beta_2 & \cdots & \cdots & 0 & 0 \\ 0 & 0 & \cdots & \cdots & -\beta_{n-2} & 0 \\ 0 & 0 & 0 & -\beta_{n-2} & E-\alpha_{n-1} & -\beta_{n-1} \\ 0 & 0 & 0 & 0 & -\beta_{n-1} & E-\alpha_n-\Sigma_2 \end{pmatrix}, \tag{18}$$

Besides, according to the definition of Green's function one can prove the following identity

$$\frac{\delta G_{st}(x_\alpha, x_\beta)}{\delta U(x)} = \sum_m G_{sm}(x_\alpha, x)\, G_{mt}(x, x_\beta). \tag{12}$$

Applying this relation to equation (11), we finally obtain

$$\frac{{\rm d}n_{\alpha\beta}(x)}{{\rm d}E} = -\frac{\sqrt{v_\alpha v_\beta}}{4\pi} \sum_{st,m} \Big[S^\dagger_{\alpha s,\beta t} G_{sm}(x_\alpha, x) G_{mt}(x, x_\beta) + (G_{sm}(x_\alpha, x) G_{mt}(x, x_\beta))^\dagger S_{\alpha s,\beta t} \Big]. \tag{13}$$

Hence, if we know Green's function of the system, we can calculate the weakly nonlinear coefficients based on equations (3, 4, 9, 10, 13).

In the above expression, the weakly linear and nonlinear coefficient $G_{\alpha\beta}(0)$ and $G_{\alpha\beta\gamma}(0)$ take values at zero frequency, which corresponds to the dc transport. In the ac case, we should consider the admittance matrix $G_{\alpha\beta}(\omega) = \delta I_\alpha / \delta V_\beta$, which represents the linear response of the current δI_α through contact α for a small voltage oscillation in reservoir β. For low frequency case, it can be further simplified as

$$G_{\alpha\beta}(\omega) = G_{\alpha\beta}(0) - {\rm i}\omega E_{\alpha\beta}, \tag{14}$$

where $E_{\alpha\beta}$ is the emittance matrix. By using the partial local density of states and characteristic potential, the emittance has the following expression

$$E_{\alpha\beta} = e^2 \left(\frac{{\rm d}N_{\alpha,\beta}}{{\rm d}E} - \int {\rm d}x \frac{{\rm d}n_\alpha(x)}{{\rm d}E} u_\beta(x) \right), \tag{15}$$

where

$$\frac{{\rm d}N_{\alpha\beta}}{{\rm d}E} = \int {\rm d}x \frac{{\rm d}n_{\alpha,\beta}(x)}{{\rm d}E} \tag{16}$$

is the space integral of partial local density of states.

The correlation of interaction to a charge particle with spin includes two categories: the charge-charge correlation and the spin-spin correlation. The charge-charge interaction in Büttiker's theory is considered through Hartree approximation and Poisson equation by which the displacement current is induced, which assures the conservation of current and gauge invariance. The spin-spin interaction is approximated by an effective magnetic field (*i.e.* the molecular field), which originates from the average of spin-spin interactions, and the spin screening is approximately contained in the molecular field that felt by a single spin. This approximation is also adopted in Slonczewski's theory, which can be used to handle the spin transport problem well. As the spin indices appeared in the Poisson equation are summed over, we think in this sense that spins also contribute to the displacement current. The spin-spin interaction leads to the exchange coupling and the spin current. In the presence of voltage V, there will be along with the electricity flowing through the barrier and energy dissipation. In reality, the spin-orbit and dipolar process internal to the magnet will cause magnetic order parameter relax very rapidly toward equilibrium. However, the purpose of this paper is to study the dc and ac conservative electric current (particle current and displacement current) originated from electron-electron interaction in the tunneling junction, so we shall not address the subject of exchange coupling and spin current in this paper, which we will discuss in future papers.

In order to calculate Green's function in equation (13), the tight-binding approximation method (or the method of finite difference) [13] is adopted in our treatment. In this way, if we choose a discrete lattice whose points are located at $x = ja$, j being an integer ($j = 1 \cdots N$), then Green's function with spin can be expressed as

$$G = (E - H_{\rm c} - \Sigma)^{-1} \tag{17}$$

where $H_{\rm c}$ is the Hamiltonian of the isolated system, and Σ is the self-energy which comes from the contribution of the leads. In real space, the matrix $E - H_{\rm c} - \Sigma$ can be expressed as

See equation (18) above

where $\beta_i = -tI$, $t = \hbar^2/2ma^2$ (a is the lattice spacing), $\alpha_j = 2tI + M_j$, $I = \begin{pmatrix} 1 & 0 \\ 0 & 1 \end{pmatrix}$ and M_j is the spin dependent potential. If $U(x)$ is the electrostatic potential in the system and $\mathbf{h}(x) = (h_1(x), h_2(x), h_3(x))$ is the molecular field in the ferromagnet, then the matrix M_j can be expressed as

$$M_j = \begin{pmatrix} U(ja) & 0 \\ 0 & U(ja) \end{pmatrix} + \begin{pmatrix} h_3(ja) & h_1(ja) - ih_2(ja) \\ h_1(ja) - ih_2(ja) & -h_3(ja) \end{pmatrix}. \tag{19}$$

In our model, the contribution to the self-energy is from the two leads [13]. If we assume that the two leads have the same polarization direction, the self-energy terms in matrix form can be written as follows:

$$\Sigma_1 = \Sigma_2 = \begin{pmatrix} -t\exp({\rm i}k_\uparrow a) & 0 \\ 0 & -t\exp({\rm i}k_\downarrow a) \end{pmatrix} \tag{20}$$

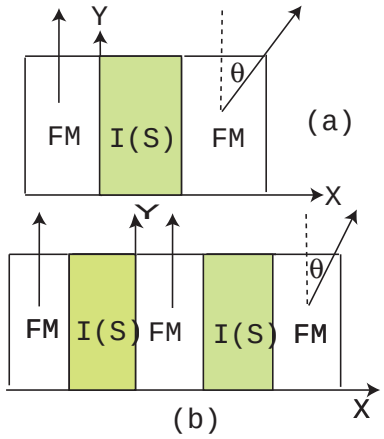

Fig. 1. The structures of single (a) and double (b) tunneling junctions.

where the wave vectors $k_{\uparrow,\downarrow}$ are determined by the dispersion relation $E \mp h_0 = 2t(1 - \cos k_{\uparrow,\downarrow}a)$, where h_0 is the polarized molecular field in the leads. If the spin polarization direction in two leads differs by an angle θ_0, the self energy Σ_1 and Σ_2 have the form of

$$\Sigma_1 = \begin{pmatrix} -t\exp(\mathrm{i}k_\uparrow a) & 0 \\ 0 & -t\exp(\mathrm{i}k_\downarrow a) \end{pmatrix},$$

$$\Sigma_2 = \Re \begin{pmatrix} -t\exp(\mathrm{i}k_\uparrow a) & 0 \\ 0 & -t\exp(\mathrm{i}k_\downarrow a) \end{pmatrix} \Re^\dagger, \quad (21)$$

where the rotation matrix $\Re$ is

$$\Re = \begin{pmatrix} \cos(\theta_0/2) & \sin(\theta_0/2) \\ -\sin(\theta_0/2) & \cos(\theta_0/2) \end{pmatrix}. \quad (22)$$

Clearly, once we obtain Green's function from the tight-binding approximation, we can calculate the weakly nonlinear coefficient and low frequency emittance coefficient by equations (4) and (15).

3 Numerical analysis

Take $Fe/Al_2O_3(MgO)/Fe$ single junction and $Fe/Al_2O_3(MgO)/Fe/Al_2O_3(MgO)/Fe$ double junction in Figure 1 as example. Let us calculate the tunneling coefficients of weakly nonlinear dc-transport and linear low frequency ac transport. For convenience, we neglect the difference of electron effective masses in barriers and ferromagnets, and treat them as the bare electron mass m_e.

We have assumed that the molecular field are zero (thus $\theta_0 = 0$) in the leads in order that the self-energy terms are simplified. In order to ensure the validity of results, we have numerically checked the unitary properties of the scattering matrix as well as the consistency of the total density of states from two methods, namely the current conservation and the gauge invariance condition.

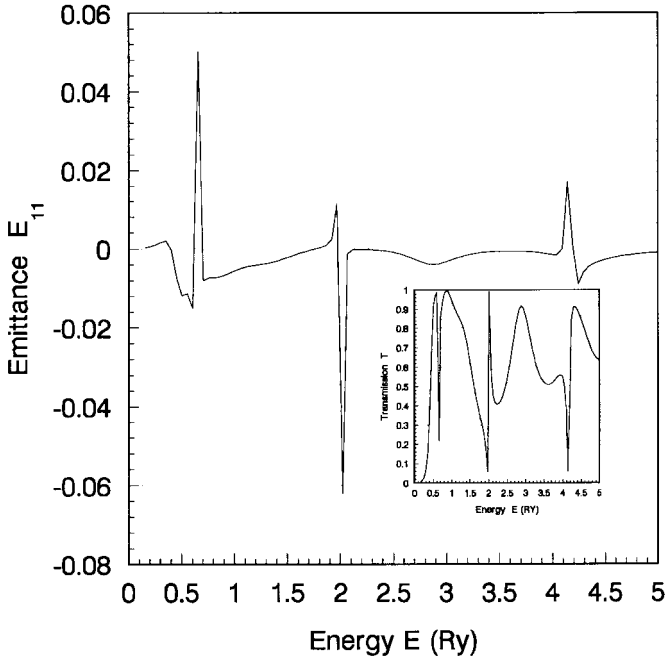

Fig. 2. The emittance coefficient and the transmission (inset) of single junction *vs.* energy, where $\theta = \pi/5$, the amplitude of the molecular field is taken to be 9.0 Ry , and $U = 0.2$ Ry.

3.1 Single junction

Consider a single junction (*e.g.* $Fe/Al_2O_3(MgO)/Fe$) whose structure is depicted in Figure 1a.

We take the width of left and right Fe layers to be 2.0 nm and 6.0 nm, respectively, and the width of the $Al_2O_3(MgO)$ layer to be 4.0 nm. For the sake of simplicity, the magnitude of the molecular field **h** in both Fe layers is assumed to be 9.0 Ry, and the barrier height in the insulator is supposed to be 0.2 Ry.

With these given conditions, we obtained the transmission coefficient defined by $T = \Sigma_{s,t}|S_{1s,2t}|^2$ and the low frequency emittance coefficient E_{11} as a function of electron energy E when the direction of the molecular field **h** in the right Fe layer is assumed to deviate from the y-axis by an angle $\theta = \pi/5$, as shown in Figure 2. It can be seen that E_{11} has sharp resonant peaks at certain energies 0.7 Ry, 2.0 Ry, 4.1 Ry and so on, which is the quantum-mechanical characteristics of the single-electron tunneling, and it is almost vanishing at energies away from the resonant points. The transmission coefficient T oscillates with energy and it also has sharp resonant peaks at the same energies. We noted that the value of T is mainly controlled by the height of the barrier. If we lower the barrier, T could exceed 1 but smaller than 2. When we adopt a small barrier (0.2 Ry) and a large molecular field in the ferromagnet (9.0 Ry), we will obtain a resonance tunneling structure shown in Figure 2. In this resonance case, the curve contains sharp peaks obviously. If the barrier and the molecular field deviate slightly from the data used above, the sharp peaks get broadened and smeared, and the curves with more small peaks become irregular compared to those in the resonant structure. The number

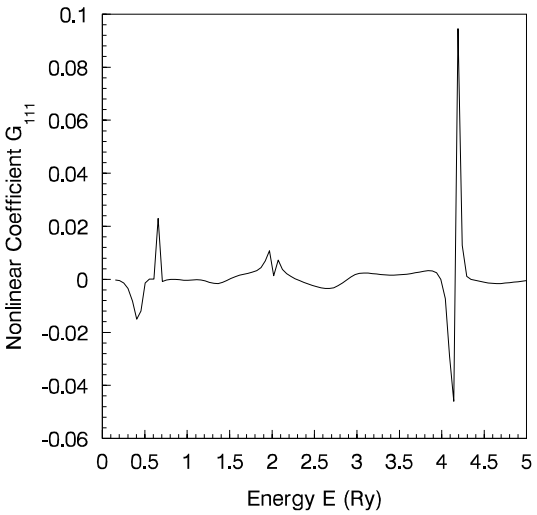

Fig. 3. The second weakly nonlinear coefficient of single junction *vs.* energy, where $\theta = \pi/5$, the amplitude of the molecular field is taken to be 9.0 Ry, and $U = 0.2$ Ry.

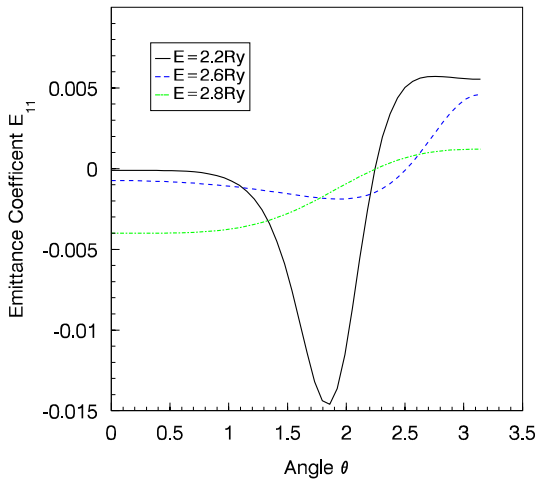

Fig. 4. The emittance coefficient of single junction *vs.* angle θ at energies 2.2 Ry, 2.5 Ry, 2.8 Ry.

of the peaks is mainly affected by the width of the barrier. A larger width of the barrier will cause more sharp peaks in the curve. When we choose the insulator barrier to be 4.0 Ry and the magnitude of the molecular field in the two ferromagnets to be 0.2 Ry, we found another resonance structure in which much more sharp peaks appear. In this latter structure, with increasing energy the amplitude of the peaks of the transmission T is also increasing, and the emittance coefficient is nearly always negative, which indicates that the junction have good transmissions. In the above case, we considered an asymmetric structure in the sense that the magnitude of the molecular field or the width of the ferromagnetic layer in the right is different from that in the left. However, if we adopt a symmetric structure, *i.e.*, both ferromagnets are the same, we see that the resonance phenomenon becomes more apparent, and the shapes of the emittance peaks at resonant points also become symmetric.

The second-order weakly nonlinear coefficient as a function of energy is presented in Figure 3. As a rectification coefficient, the second-order weakly nonlinear conductance is small compared with the transmission coefficient, and it shows sharp peaks at energies 0.7 Ry, 2.0 Ry, 4.1 Ry and so on which just correspond to the energies at the resonant points of the transmission coefficient. Away from these resonant points, G_{111} is almost vanishing. From the figure it can be observed that the amplitudes of the resonances are small at 0.7 and 2.0 Ry, but the resonant amplitude at 4.1 Ry is about 4 times greater than the other two, showing the dominance of the nonlinear effect at this specific energy. Owing to the requirement of current conservation and gauge invariance, the second-order nonlinear conductance should identically vanish in the symmetric case because it is antisymmetric when exchanging the indices. If we choose the molecular field and the width of the ferromagnets in the left and right to be the same (*i.e.*, a symmetric case) in our numerical computation, the second-order nonlinear conductance is indeed zero, which confirms the correctness of our method. Besides, for an asymmetric case in which there are different molecular fields or widths in the left and right ferromagnets, we observed that the second-order nonlinear conductance is not zero, and exhibits resonant peaks at energies 0.7 Ry, 2.0 Ry, 4.1 Ry and so on. The height of the resonance peak is mainly affected by the magnitude of the molecular field, and the number of peaks is also controlled by the width of the ferromagnets. Certainly, the height and width of the insulator barrier also have some effects on the second-order nonlinear coefficient like on the emittance coefficient. According to the current conservation and gauge invariance condition, if we transpose the asymmetric left and right ferromagnet in the junction, the second-order weakly nonlinear coefficient should be antisymmetric, which is supported by our numerical results. Note that the curves of G_{111} in the two (*i.e.* untransposed and transposed) asymmetric cases are symmetric about the energy axis. However, this observation is not suitable to the emittance coefficient which dose not alter if transposed. The emittance coefficient also possesses more obvious resonance peaks in the symmetric case than in the asymmetric case, and it is certainly nonzero in the symmetric case.

Figures 4 and 5 show the low frequency emittance coefficient and the second-order weakly nonlinear coefficient in single junction as a function of angle θ which determines the direction of the molecular field. In each figure, we plot three different curves for energies 2.2 Ry, 2.8 Ry, 2.5 Ry which correspond to the energies at the bottom, the top and the point between the top and the bottom, respectively. The variation tendency of the curves with θ is different for different energies, which is due to the different reflection coefficients at these energies. E_{11} has a deep ditch around $\theta \approx 3\pi/5$ at energy 2.2 Ry. With increasing energy, the ditch is gradually smeared out and becomes a bit flat, and when the energy is greater than 2.8 Ry, E_{11} becomes a monotonically increasing function of θ.

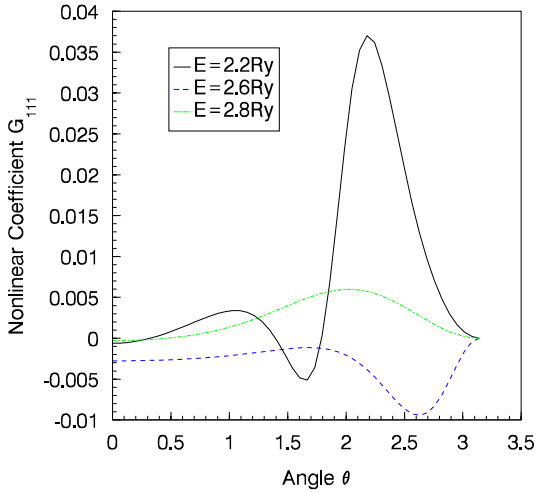

Fig. 5. The second weakly nonlinear coefficient of single junction *vs.* angle θ at energies 2.2 Ry, 2.5 Ry, 2.8 Ry.

The curve which has relatively small value corresponds to the case with a small reflection coefficient in Figure 4. G_{111} as a function of θ has one small peak around $\theta = 0.4\pi$ and one sharp peak around $\theta = 0.7\pi$ at energy 2.2 Ry. With increasing energy, the small peak get broadened and the sharp peak becomes a round ditch. At the energy greater than 2.8 Ry, the small peak get more round and the ditch disappears for $\theta \leq \pi$. In the resonant structure case, both the weakly nonlinear coefficient and the emittance coefficient vary with θ obviously. If we change the molecular field in ferromagnets or the height of the barrier slightly away from this resonance point, the variation with θ will become slower compared with the resonance case. When we choose the molecular field in the left and right ferromagnets very small (0.2 Ry), and the height of the insulator barrier larger (1.3 Ry), the variation of the weakly nonlinear coefficient G_{111} and the emittance coefficient E_{11} are very slight. In the asymmetric structure case in which the left and right ferromagnets have different widths or molecular fields, the nonlinear coefficient varies obviously. If we exchange the asymmetric left and right ferromagnets, then the curves will be symmetric about the θ axis in the two cases due to the current conservation and gauge invariance condition. However, the emittance coefficient varies more obviously with θ in the symmetric structure than in the asymmetric case.

3.2 Double junction

Let us now consider a double junction (*e.g.* Fe/Al_2O_3(MgO)/Fe/Al_2O_3(MgO)/Fe) whose structure is shown in Figure 1b. We assume that the widths of the first, second and third Fe layers are 2.0 nm, 2.0 nm and 5.0 nm, respectively, and the widths of the first and the second Al_2O_3(MgO) layer are 4.0 nm and 4.0 nm, respectively. The magnitude of the molecular field **h** in the ferromagnet is taken to be 9.0 Ry, and the barrier height in the insulator is supposed to be 0.2 Ry.

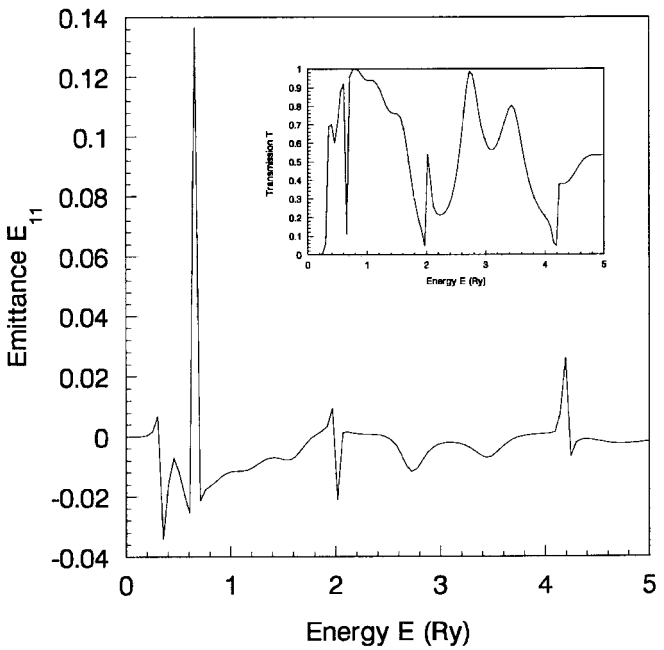

Fig. 6. The emittance coefficient and the transmission (inset) of double junction *vs.* energy, where $\theta = \pi/5$, the amplitude of the molecular field is taken to be 9.0 Ry, and $U = 0.2$ Ry.

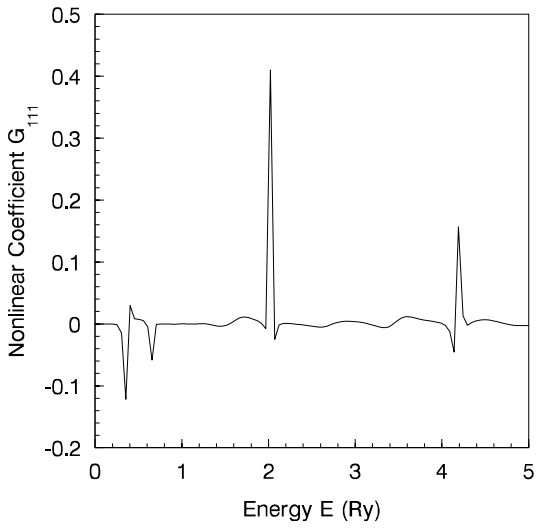

Fig. 7. The second weakly nonlinear coefficient of double junction *vs.* energy, where $\theta = \pi/5$, the amplitude of the molecular field is taken to be 9.0 Ry, and $U = 0.2$ Ry.

For the double junction, we calculated the low frequency emittance coefficient and the second-order weakly nonlinear coefficient as a function of energy when the direction angle of the molecular field in the right ferromagnet is assumed to be $\theta = \pi/5$. The results are shown in Figures 6 and 7, respectively. It is seen that the weakly nonlinear coefficient, the emittance coefficient and the transmission as a function of energy are generally similar to those in the single junction case, but they have more peaks than in the single junction, which means that more resonances may appear in the double junction. Apart from

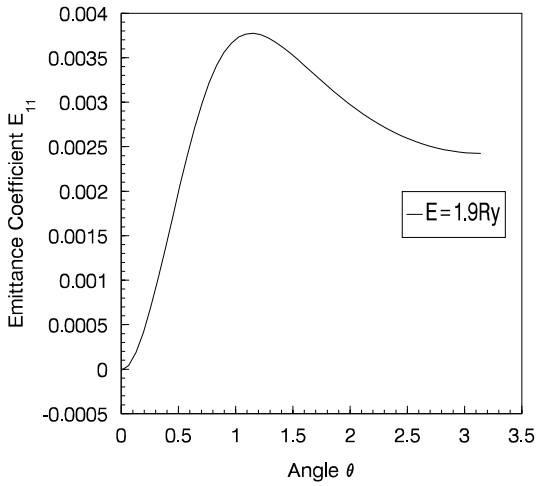

Fig. 8. The emittance coefficient of double junction *vs.* angle θ at energy 1.9 Ry.

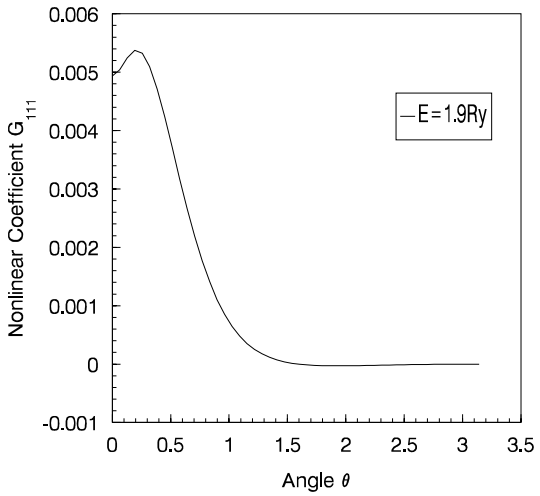

Fig. 9. The second weakly nonlinear coefficient of double junction *vs.* angle θ at energy 1.9 Ry.

this difference, E_{11} has a more sharp resonance peak at $E \sim 0.7$ Ry whose amplitude is about twice greater than that in the single junction, while the peak at $E \sim 2.0$ Ry is just about twice smaller than that in the single junction. The transmission coefficient exhibits resonance peaks at energies 0.5 Ry, 0.7 Ry, 2.0 Ry, 4.1 Ry and so on, which is quite similar to the result in the single junction. In addition, it is surprising to see that G_{111} has a ditch at $E \sim 0.7$ Ry but in the single junction it is a peak at the same energy, and also, G_{111} has a very sharp peak at $E \sim 2.0$ Ry but in the single junction it is a small ditch at the corresponding energy. The resonances at $E \sim 4.1$ Ry are comparable for both kind of junctions. The second-order weakly nonlinear coefficient and the emittance coefficient show resonance peaks at the same energies as for the transmission coefficient. If we alter either the barrier height, the molecular field or the width of the junction, the curves will vary like in the single junction case. The variation of the emittance coefficient and the weakly nonlinear coefficient with θ are shown in Figures 8 and 9, respectively. At $E = 1.9$ Ry, E_{11} increases with θ and reaches to a maximum around $\theta = 2\pi/5$ and then decreases till $\theta = \pi$, while at the same energy G_{111} increases with θ and quickly reaches to a small maximum around $\theta = 0.1\pi$ and then decreases to zero around $\theta = \pi/2$. For $\theta \in [\pi/2, \pi]$, G_{111} is identically vanishing. It is obvious that the weakly nonlinear coefficient (though small) and the emittance coefficient are strongly dependent on the direction of the molecular field in the right ferromagnetic layer. Besides, we noted that the values of G_{111} and E_{11} are mainly affected by a proper combination of parameters (*i.e.* the magnitudes of the molecular fields and the widths of the ferromagnetic layers, the widths and the height of the insulating barrier) which gives the resonant structure. If the parameters deviate from the resonant structure, G_{111} and E_{11} become smaller.

In Figures 6 and 7, we have assumed that the molecular fields in the first and second ferromagnets are aligned along the y-axis, and the angle between the y-axis and the molecular field in the third ferromagnet is fixed as $\pi/5$. However, if we let the molecular field in the second ferromagnet have an angle $\pi/5$ from the y-axis, and the first and third molecular fields are parallel to the y-axis, the curves of the emittance coefficient and the weakly nonlinear coefficient just have a little change compared with the curves in Figures 6 and 7. It appears that they do not depend obviously on in which ferromagnet the direction of the molecular field deviates from the y-axis. In this case, if we set the width of the third ferromagnet to be the same as that of the first and the second ferromagnets (2 nm), and the angle θ is in the second ferromagnet, namely, this structure is symmetric in geometry but is not symmetric in whole because of the aligned molecular field in the second ferromagnet, we will see that the second weakly nonlinear coefficient is nearly zero, which means that the asymmetry caused by the aligned angle of the molecular field is weak, and contributes very small to the second-order weakly nonlinear coefficient. This case is similar to the case in which we choose the aligned angle in the third ferromagnet. When the molecular field in the first ferromagnet is parallel to the y-axis, but in the second ferromagnet it is antiparallel to the y-axis, and the aligned angle ($\pi/5$) is assumed in the third ferromagnet, we observed that both the transmission and the second weakly nonlinear coefficient are very small in magnitude compared with those in Figures 6 and 7. In this case, it is not easy for transmitting. Moreover, there is another resonant structure caused by the barrier in the insulator. When we chose the molecular field in the first, second and third ferromagnets very small (0.2 Ry), and the barrier in the insulator relatively large (1.2 Ry), that will form another resonant structure, we found that the transmission coefficient oscillates obviously, and has an increasing tendency with energy, whose maximums can approach 2. The emittance coefficient and the weakly nonlinear coefficient also have their own resonant peaks.

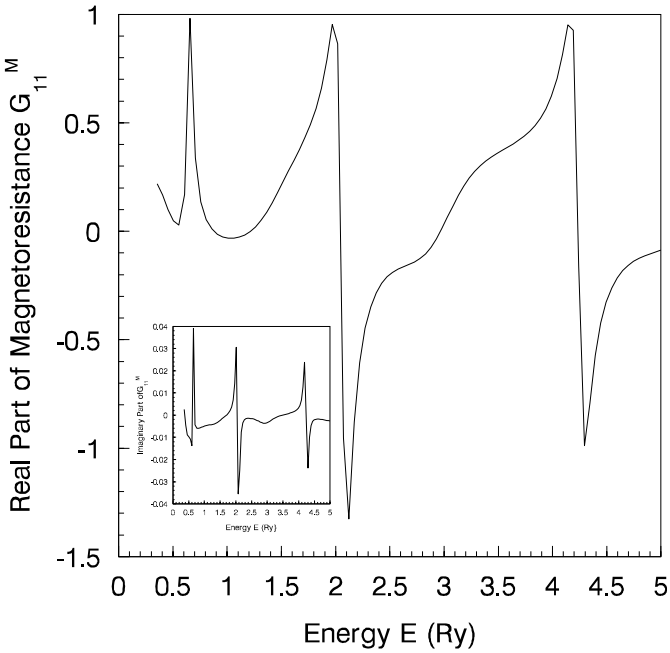

Fig. 10. The real part and the imaginary part (inset) of ac tunneling magnetoresistance $G_{11}^{M}(\theta,\omega)$ of single junction *vs.* energy, where $\theta = \pi/5$, $\omega = 1$ Hz.

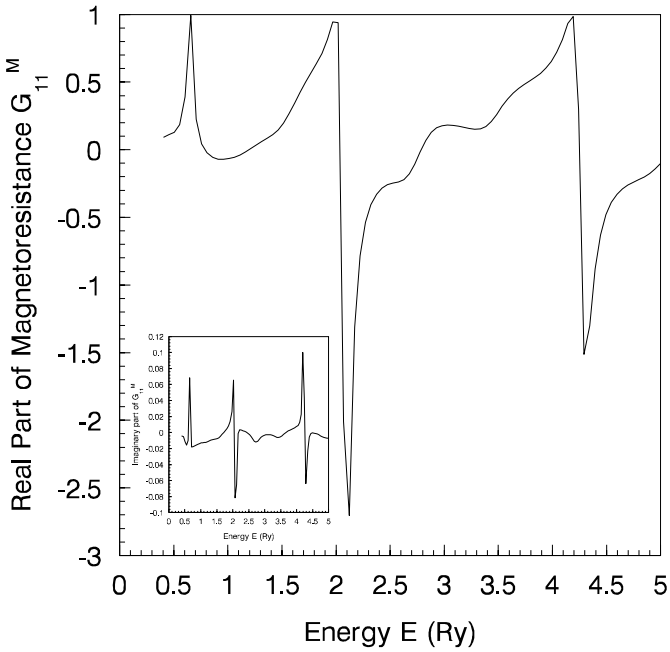

Fig. 11. The real part and the imaginary part (inset) of the ac tunneling magnetoresistance $G_{11}^{M}(\theta,\omega)$ of double junction *vs.* energy, where $\theta = \pi/5$, $\omega = 1$ Hz.

3.3 AC tunneling magnetoresistance

The AC tunneling magnetoresistance can be defined as usual as: $G_{\alpha\beta}^{M}(\theta,\omega) = \frac{G_{\alpha\beta}^{\uparrow\uparrow}(\omega) - G_{\alpha\beta}^{\theta}(\omega)}{G_{\alpha\beta}^{\uparrow\uparrow}(\omega)}$, which is a function of θ and frequency ω, where θ is the angle between the molecular fields in two different magnetic layers. Generally, $G_{11}^{M}(\theta,\omega)$ is complex. In Figure 10, we present the tunneling magnetoresistance $G_{11}^{M}(\theta,\omega)$ defined above as a function of energy E for a single junction at $\theta = \pi/5$ and $\omega = 1$ Hz. It is seen that the imaginary part of TMR is very small. At the resonance points 0.6 Ry, 2.0 Ry, 4.1 Ry, and so on, $G_{11}^{M}(\theta,\omega)$ approaches its maximum values. For other θ and ω, we observed a similar structure of curves besides slight changes of the magnitudes. $G_{11}^{M}(\theta,\omega)$ as a function of energy for a double junction is given in Figure 11. One may see that the curves show a very similar structure as that in the single junction except a small peak appeared at energy 3.0 Ry. We also studied the variation of the tunneling magnetoresistance $G_{11}^{M}(\theta,\omega)$ for single and double junctions with θ, and the results are shown in Figures 12 and 13, respectively. For a single junction, at given energy 2.8 Ry and $\omega = 1$ Hz we found that the curves of the real and imaginary parts of $G_{11}^{M}(\theta,\omega)$ have a similar structure in shape, namely, with increasing θ it decreases from zero and arrives at a round minimum and then increases to a maximum. For a double junction, at energy 1.9 Ry and $\omega = 1$ Hz the real part of $G_{11}^{M}(\theta,\omega)$ increases with increasing θ, and finally saturates around $\theta = \pi$, while the imaginary part first increases with increasing θ and reaches to a maximum and then decreases. For both junctions the real part of $G_{11}^{M}(\theta,\omega)$ is about two orders

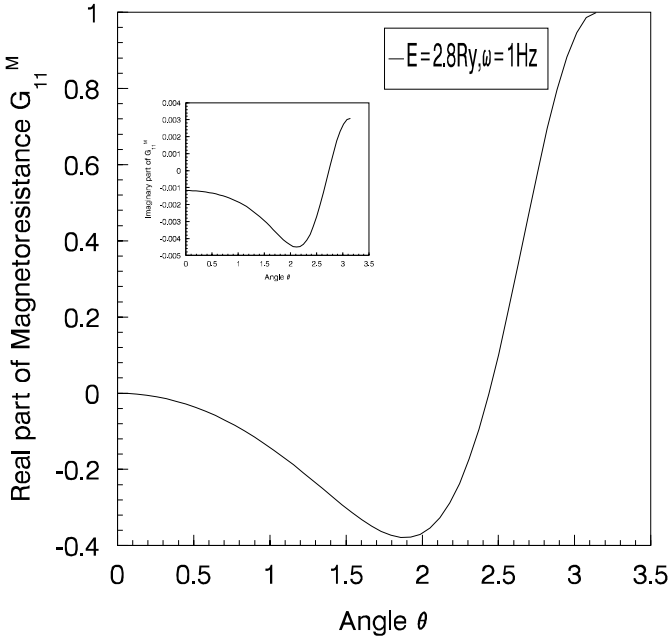

Fig. 12. The real part and the imaginary part (inset) of the ac tunneling magnetoresistance $G_{11}^{M}(\theta,\omega)$ of single junction *vs.* θ, where $E = 2.8$ Ry, $\omega = 1$ Hz.

larger than the imaginary part. By definition, $G_{11}^{M}(\theta,\omega)$ as a function of θ has a close relationship with the emittance coefficient, and the behaviors of the latter determine ones of the former. Furthermore, we noted that different energies generate different behaviors, and with increasing frequency $G_{11}^{M}(\theta,\omega)$ is almost linearly decreasing at given energy and θ.

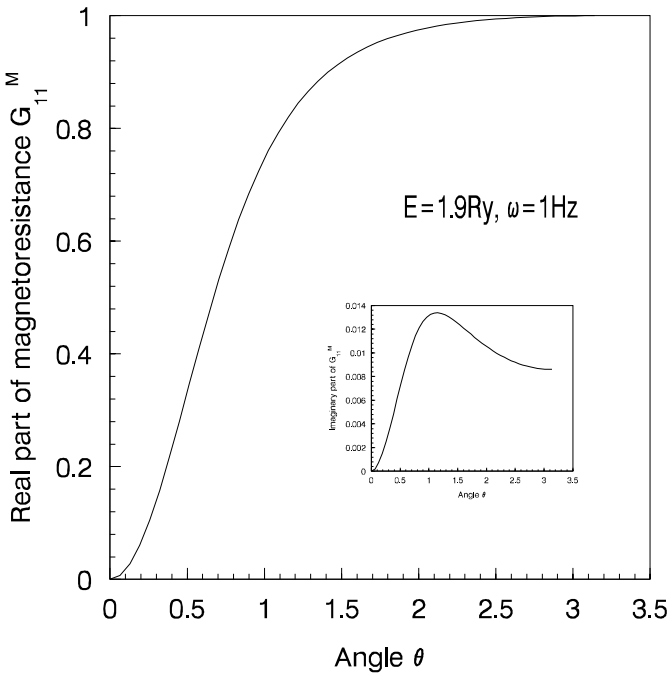

Fig. 13. The real part and the imaginary part (inset) of the ac tunneling magnetoresistance $G_{11}^{M}(\theta,\omega)$ of double junction *vs.* θ, where $E = 1.9$ Ry, $\omega = 1$ Hz.

4 Summary

Based on Büttiker gauge invariant, charge conservation, nonlinear transport theory, we have studied the weakly nonlinear dc transport coefficient and the linear low frequency transport coefficient for spin polarized tunneling of ferromagnet/insulator(semiconductor) single and double junctions. Both the nonlinear coefficient and the emittance coefficient as a function of energy and the aligned angle θ of the molecular fields in ferromagnetic layers are explored in many cases such as changing the lengths of ferromagnet and insulator layers, the height of the barrier, the magnitudes of the molecular field, etc. We have observed that the variation of the two coefficients are mainly determined by the resonant structure. The symmetric and asymmetric structures also have obvious influences on them, and the double junction is affected more than the single junction. Finally, we discussed the ac tunneling magnetoresistance for the single and double junctions. In our model, some important factors such as the crystal potential, spin waves, inelastic tunnelings, the difference of the electron effective masses in ferromagnets and insulator, and so on are not considered. The Green function for the spin-polarized tunneling is obtained by the tight-binding approximation, which could be further improved by other methods. On the other hand, our discussion is only limited to zero temperature. How to extend our consideration to finite temperature is an open question, which will be left for study in future.

This work is supported in part by NSFC, Climbing Project of China, and State Key Project for Fundamental Research of China.

References

1. J.S. Moodera, L.R. Kinder, T.M. Wong, R. Meservey, Phys. Rev. Lett. **74,** 3273 (1995).
2. J.S. Moodera, L.R. Kinder, J. Appl. Phys. **79**, 4724 (1996).
3. T. Miyazaki, N. Tezuka, J. Magn. Magn. Matter. **139,** L231 (1995).
4. N. Tezuka, T. Miyazaki, J. Appl. Phys. **79**, 6262 (1996).
5. J.C. Slonczewski, Phys. Rev. B **39,** 6995 (1989).
6. X.D. Zhang, B.Z. Li, G. Sun, F.C. Pu, Phys. Rev. B **56**, 5484 (1997).
7. Y. Li, B.Z. Li, W.S. Zhang, D.S. Dai, Phys. Rev. B **57**, 1079 (1998).
8. G.E.W. Bauer, Phys. Rev. Lett. **69,** 1676 (1992).
9. A. Brataas, Yu. V. Nazarov, G.E.W. Bauer, Phys. Rev. Lett. **84**, 2481 (2000).
10. M. Büttiker, J. Phys. Cond. Matt. **5,** 9361 (1993).
11. T. Christen, M. Büttiker, Europhys. Lett. **53**, 523 (1996).
12. T. Christen, M. Büttiker, Phys. Rev. Lett. **77**, 143 (1996).
13. S. Datta, *Electronic Transport in Mesoscopic Systems* (Cambridge University Press, 1995).
14. J. Wang, H. Guo, Phys. Rev. B **54,** R11090 (1996).
15. Z.S. Ma, J. Wang, H. Guo, Phys. Rev. B **57**, 9108 (1998); Z.S. Ma, J. Wang, H. Guo, Phys. Rev. B **59**, 7575 (1999).
16. J. Wang, H. Guo, J.L. Mozos, C.C. Wan, G. Taraschi, Q.R. Zheng, Phys. Rev. Lett. **80**, 4277 (1998).
17. J. Wang, Q.R. Zheng, H. Guo, Phys. Rev. B **55,** 9770 (1997); J. Wang, Q.R. Zheng, H. Guo, Phys. Rev. B **55,** 9763 (1997).
18. Q.R. Zheng, J. Wang, H. Guo, Phys. Rev. B **56**, 12462 (1997).
19. W.D. Sheng, Q.R. Zheng, J. Wang, H. Guo, Phys. Rev. B **59**, 538 (1999).